

Microwave background anisotropies from Alfvén waves

R. Durrer

Département de Physique Théorique, Université de Genève, 24 quai Ernest Ansermet, CH-1211 Genève 4, Switzerland

T. Kahniashvili

Department of Theoretical Astrophysics, Abastumani Astrophysical Observatory, Kazbegi Avenue 2a, 380060, Tbilisi, Georgia

A. Yates

Département de Physique Théorique, Université de Genève, 24 quai Ernest Ansermet, CH-1211 Genève 4, Switzerland

(Received 9 July 1998; published 17 November 1998)

We investigate microwave background anisotropies in the presence of primordial magnetic fields. We show that a homogeneous field with fixed direction can amplify vector perturbations. We calculate the correlations of $\delta T/T$ explicitly and show that a large scale coherent field induces correlations between $a_{l-1,m}$ and $a_{l+1,m}$. We discuss constraints on the amplitude and spectrum of a primordial magnetic field imposed by observations of CMB anisotropies. [S0556-2821(98)06224-9]

PACS number(s): 98.70.Vc, 98.62.En

I. INTRODUCTION

Since the detection of cosmic microwave background (CMB) anisotropies by the Cosmic Background Explorer (COBE) satellite [1], it has become clear that anisotropies in the CMB provide a powerful tool for distinguishing models of cosmological structure formation. Furthermore, they may help to determine cosmological parameters which influence their spectrum in a well defined, non-trivial way [2]. It is thus important to calculate the CMB anisotropies for a given model simply and reliably.

The origin of observed galactic magnetic fields of the order of μG is still unknown. For some time it has been believed that tiny seed fields can be amplified by a non-linear galactic dynamo mechanism. The effectiveness of this process has recently been strongly questioned, however [3]. If magnetic fields are not substantially amplified by non-linear effects, but have just contracted with the cosmic plasma during galaxy formation, primordial fields of the order 10^{-9} G on megaparsec scales are required to induce the observed galactic fields.

It is interesting to note that a field strength of 10^{-8} G provides an energy density of $\Omega_B = B^2/(8\pi\rho_c) \sim 10^{-5}\Omega_\gamma$, where Ω_γ is the density parameter in photons. We naively expect a field of this amplitude to induce perturbations in the CMB on the order of 10^{-5} , which is just the level of the observed anisotropies. This leads us to investigate the extent to which the isotropy of the CMB may constrain primordial magnetic fields. It is clear from our order of magnitude estimate that we shall never be able to constrain tiny seed fields on the order of 10^{-13} G with this approach, but primordial fields of 10^{-9} to 10^{-8} G may well have left observable traces in the microwave background.

This is the question we investigate quantitatively in this paper. Some work on the influence of primordial magnetic fields on CMB anisotropies has already been published, particularly the cases of fast magneto-sonic waves and the gravitational effects of a constant magnetic field [6–8]. Here we study Alfvén waves. We leave aside the problem of gen-

eration of primordial magnetic fields. This issue is addressed e.g. in [4,5].

The possible influence of magnetic fields on large scale structure formation has been investigated in [9] and references therein.

The paper is organized as follows. In Sec. II we discuss the effect of a homogeneous magnetic field background on the cosmic plasma. Both scalar (potential, or fast and slow magneto-sonic waves) and vorticity (Alfvén) waves can be induced. We study the latter. In Sec. III we consider the influence of Alfvén waves on CMB anisotropies. The influence of the magneto-sonic waves can be interpreted as a slight change in the speed of sound, and has been investigated in [6]. In Sec. IV we present our conclusions. Some of the more technical computations as well as a discussion of Silk damping of vector perturbations are left to two appendices.

Notation. For simplicity we concentrate on the case $\Omega_0 = 1$. The choice of Ω is of little importance for our perturbation variables (which have to be calculated for at early times, when curvature effects are not significant), but does influence the resulting C_l 's due to projection effects. Throughout, we use conformal time which we denote by t . The unperturbed metric is thus given by $ds^2 = a^2(t)(-dt^2 + \delta_{ij}dx^i dx^j)$. Greek indices run from 0 to 3, Latin ones from 1 to 3. We denote spatial (3d) vectors with bold face symbols.

II. COSMOLOGICAL VECTOR PERTURBATIONS AND ALFVÉN WAVES

Vector perturbations of the geometry are of the form

$$(h_{\mu\nu}) = \begin{pmatrix} 0 & B_i \\ B_j & H_{i,j} + H_{j,i} \end{pmatrix}, \quad (1)$$

where \mathbf{B} and \mathbf{H} are divergence-free, 3d vector fields supposed to vanish at infinity. Studying the behavior of these variables under infinitesimal coordinate transformations

(called gauge transformations in the context of linearized gravity), one finds that the combination

$$\boldsymbol{\sigma} = \dot{\mathbf{H}} - \mathbf{B} \quad (2)$$

is gauge invariant. Geometrically, $\boldsymbol{\sigma}$ determines the vector contribution to the perturbation of the extrinsic curvature [10,11].

To investigate perturbations of the energy-momentum tensor, we consider a baryon, radiation and cold dark matter (CDM) universe for which anisotropic stresses are negligible. The only vector perturbation in the energy-momentum tensor is thus a perturbation of the energy flux, u , the time-like eigenvector of T^ν_μ . We parametrize a vector perturbation of u with a divergence free vector field \mathbf{v} , such that

$$\mathbf{u} = \frac{1}{a} \mathbf{v}. \quad (3)$$

Analyzing the gauge transformation properties of \mathbf{v} , one finds two simple gauge-invariant combinations [10],

$$\mathbf{V} = \mathbf{v} - \dot{\mathbf{H}} \quad \text{and} \quad \boldsymbol{\Omega} = \mathbf{v} - \mathbf{B}. \quad (4)$$

They are simply related by

$$\mathbf{V} = \boldsymbol{\Omega} - \boldsymbol{\sigma}. \quad (5)$$

The perturbations of the Einstein equations, together with energy-momentum conservation, yield [11]

$$-\frac{1}{2} \Delta \boldsymbol{\sigma} = 3 \left(\frac{\dot{a}}{a} \right)^2 \boldsymbol{\Omega}, \quad (6)$$

$$\dot{\boldsymbol{\sigma}} + 2 \left(\frac{\dot{a}}{a} \right) \boldsymbol{\sigma} = 0, \quad (7)$$

$$\dot{\boldsymbol{\Omega}} + (1 - 3c_s^2) \frac{\dot{a}}{a} \boldsymbol{\Omega} = 0. \quad (8)$$

The two Einstein equations (6), (7) and the momentum conservation equation (8) are not independent. Equation (8) follows from Eqs. (6) and (7).

This system clearly does not describe waves. From Eq. (7) it follows that $\boldsymbol{\sigma}$ decays like $1/a^2$. Furthermore, Eq. (6) implies $\boldsymbol{\Omega} \propto (kt)^2 \boldsymbol{\sigma}$. In the radiation dominated era, where $a \propto t$, this yields $\boldsymbol{\Omega} = \frac{1}{6} (kt_{in})^2 \boldsymbol{\sigma}_{in}$, where t_{in} is some initial time at which fluctuations were created, e.g. the end of inflation. The fact that $\boldsymbol{\Omega}$ stays constant during the radiation dominated era also follows from Eq. (8). On cosmologically interesting scales, $k \ll 1/t_{in}$, we have therefore $\boldsymbol{\Omega} \ll \boldsymbol{\sigma}_{in}$ and $\boldsymbol{\sigma} \ll \boldsymbol{\sigma}_{in}$. In contrast, scalar and tensor perturbations remain constant on super-horizon scales. For this reason, vector perturbations induced at a very early epoch (e.g. inflation) which have evolved freely can be entirely neglected in comparison to their scalar and tensor counterparts.

This situation is altered in the presence of a primordial magnetic field, which induces vorticity waves after the inflationary era. Let us consider a homogeneous magnetic field

\mathbf{B}_0 before the time of decoupling of matter and radiation. Such a field could have originated, for example, at the electroweak phase transition [5]. When the photon-baryon fluid is taken to be a perfectly conducting plasma, an external magnetic field induces two distinct modes of oscillation. Magneto-sonic waves are scalar perturbations which propagate at speeds c_\pm slightly above or very much below the ordinary speed of sound in the plasma. These induce density oscillations just like ordinary acoustic waves. The slight change in the speed of sound can alter the position and shape of the acoustic peaks in the CMB spectrum [6]. Here, however, we discuss the vectorial *Alfvén waves*.

We assume a plasma with infinite conductivity and use the frozen-in condition

$$\mathbf{E} + \mathbf{v} \times \mathbf{B} = \mathbf{0},$$

where \mathbf{v} is the plasma velocity field. Our plasma is non-relativistic ($v \ll 1$). The field lines of a homogeneous background magnetic field in a Friedmann universe are just conformally diluted, such that $B_0 \propto 1/a^2$. Until recombination, the photon-baryon plasma is dominated by photons, $\rho_r \simeq \rho_\gamma \propto a^{-4}$ (ρ_r denotes the combined baryon and photon energy density) and the ratio $B_0^2/(\rho_r + p_r)$ is time-independent. We study purely vortical waves which induce a fluid vorticity field $\boldsymbol{\Omega}(\mathbf{k})$ normal to \mathbf{k} . We note that charged particles are tightly coupled to the radiation fluid and obey the equation of state $p_r = \rho_r/3$.

It is convenient to rescale physical quantities like the fields and the current density as follows:

$$\mathbf{E} \rightarrow \mathbf{E}a^2, \quad \mathbf{B} \rightarrow \mathbf{B}a^2 \quad \text{and} \quad \mathbf{J} \rightarrow \mathbf{J}a^3.$$

We now introduce first-order vector perturbations in the magnetic field (\mathbf{B}_1) and in the fluid velocity ($\boldsymbol{\Omega}$);

$$\mathbf{B} = \mathbf{B}_0 + \mathbf{B}_1, \quad \nabla \cdot \mathbf{B}_1 = 0 \quad \text{and} \quad (9)$$

$$\mathbf{v} = \boldsymbol{\Omega}, \quad \nabla \cdot \boldsymbol{\Omega} = 0. \quad (10)$$

To obtain the equations of motion for $\boldsymbol{\Omega}$ and \mathbf{B}_1 , we first consider Maxwell's equations. Since the fluid velocity is small, we may neglect the displacement current in Ampère's law, which then yields

$$\mathbf{J} = \frac{1}{4\pi} \nabla \times \mathbf{B}_1. \quad (11)$$

We replace \mathbf{E}_1 with \mathbf{B}_0 , using the frozen-in condition. The induction law then gives

$$\frac{\partial}{\partial t} \mathbf{B}_1 = \nabla \times (\mathbf{v} \times \mathbf{B}_0). \quad (12)$$

Inserting relation (11) for the current, the equation of motion ($T^{i\mu}_{;\mu} = F^{i\mu} j_\mu$) for vector perturbations in the plasma becomes

$$\frac{\partial}{\partial t} \mathbf{v} = - \frac{1}{4\pi(\rho_r + p_r)} \mathbf{B}_0 \times (\nabla \times \mathbf{B}_1). \quad (13)$$

(We have neglected viscosity, which is a good approximation on scales much larger than the Silk damping scale [12].) Taking the time derivative of this equation, we obtain with the help of Eqs. (9), (10) and (12) for a fixed Fourier mode \mathbf{k}

$$\dot{\mathbf{\Omega}} = \frac{(\mathbf{B}_0 \cdot \mathbf{k})^2}{4\pi(\rho_r + p_r)} \mathbf{\Omega} \quad \text{and} \quad (14)$$

$$\dot{\mathbf{\Omega}} = \frac{i\mathbf{B}_0 \cdot \mathbf{k}}{4\pi(\rho_r + p_r)} \mathbf{B}_1. \quad (15)$$

These equations¹ describe waves propagating at the velocity $v_A(\mathbf{e} \cdot \hat{\mathbf{k}})$, where

$$v_A^2 = \frac{B_0^2}{4\pi(\rho_r + p_r)}, \quad v_A \sim 4 \times 10^{-4} (B_0/10^{-9} \text{ G})$$

is the Alfvén velocity and \mathbf{e} is the unit vector in the direction of the magnetic field. Typically the Alfvén velocity will be very much smaller than the speed of acoustic oscillations in the radiation-dominated plasma ($c_s^2 = 1/3 \gg v_A^2$).

Due to the observed isotropy of the CMB, we have to constrain the magnetic field contribution to the total energy density. For example, in the radiation dominated era it must be a fraction of less than about 10^{-5} [7], leading to $v_A \lesssim 10^{-3}$. Equation (14) is homogeneous in $\mathbf{\Omega}$ and so does not determine the amplitude of the induced vorticity. The general solution contains two modes, $\cos(v_A k t \mu)$ and $\sin(v_A k t \mu)$ (where $\mu = \mathbf{e} \cdot \hat{\mathbf{k}}$). If the cosine mode is present, it dominates on the relevant scales $k < 1/(v_A t_{dec})$. Then we can approximate $\cos(v_A k t_{dec} \mu) \approx 1$ and the sine is negligibly small. But this mode then describes the usual vector perturbations without a magnetic field. We assume it to be absent. We want to consider initial conditions, then, with

$$\mathbf{\Omega}(\mathbf{k}, t=0) = 0.$$

Only the sine mode is present and we have

$$\mathbf{\Omega}(\mathbf{k}, t) = \mathbf{\Omega}_0 \sin(v_A k t \mu) \approx \mathbf{\Omega}_0 v_A k t \mu. \quad (16)$$

The initial amplitude of $\mathbf{\Omega}_0$ is connected with the amplitude of \mathbf{B}_1 by means of Eq. (15), yielding

$$|\mathbf{\Omega}_0| = (v_A/B_0) |\mathbf{B}_1|. \quad (17)$$

This allows a vorticity amplitude of up to the order of the Alfvén velocity (see also [8]).

III. CMB ANISOTROPIES FROM ALFVÉN WAVES

Vector perturbations induce anisotropies in the CMB via a Doppler effect and an integrated Sachs-Wolfe term [11]

¹Our derivation is valid either in a gauge invariant framework as outlined in [13] or in a gauge with vanishing shift vector. In other gauges metric coefficients will enter and complicate the equations.

$$\left(\frac{\Delta T}{T}\right)^{(vec)} = -\mathbf{V} \cdot \mathbf{n} \Big|_{t_{dec}}^{t_0} + \int_{t_{dec}}^{t_0} \dot{\boldsymbol{\sigma}} \cdot \mathbf{n} d\lambda, \quad (18)$$

where the subscripts dec and 0 denote the decoupling epoch ($z_{dec} \sim 1100$) and today respectively. Since the geometric perturbation $\boldsymbol{\sigma}$ is decaying, the integrated term is dominated by its lower boundary and just cancels $\boldsymbol{\sigma}$ in $\mathbf{V} = \mathbf{\Omega} - \boldsymbol{\sigma}$. Neglecting a possible dipole contribution from vector perturbations today, we obtain

$$\frac{\delta T}{T}(\mathbf{n}, \mathbf{k}) \approx \mathbf{n} \cdot \mathbf{\Omega}(\mathbf{k}, t_{dec}) = \mathbf{n} \cdot \mathbf{\Omega}_0 v_A k t_{dec} (\mathbf{e} \cdot \hat{\mathbf{k}}). \quad (19)$$

We assume that the vector perturbations $\mathbf{\Omega}_0$ are created by some isotropic random process, and so have a power spectrum of the form

$$\langle \Omega_{0i}(\mathbf{k}) \Omega_{0j}(\mathbf{k}) \rangle = (\delta_{ij} - \hat{k}_i \hat{k}_j) A(|\mathbf{k}|). \quad (20)$$

For simplicity, we further assume that the spectrum $A(k) = (1/2)|\mathbf{\Omega}_0|^2(k)$ is a simple power law over the range of scales relevant here,

$$A(k) = A_0 \frac{k^n}{k_0^{n+3}}, \quad k < k_0, \quad (21)$$

for some dimensionless constant A_0 and cutoff wave number k_0 . With this we can calculate the CMB anisotropy spectrum.

The C_l 's are defined by

$$\left\langle \frac{\delta T}{T}(\mathbf{n}) \frac{\delta T}{T}(\mathbf{n}') \right\rangle \Big|_{(\mathbf{n} \cdot \mathbf{n}' = \mu)} = \frac{1}{4\pi} \sum_l (2l+1) C_l P_l(\mu). \quad (22)$$

A homogeneous magnetic field induces a preferred direction \mathbf{e} and the correlation function (22) is no longer a function of $\mathbf{n} \cdot \mathbf{n}' = \mu$ alone but depends also on the angles between \mathbf{n} and \mathbf{B}_0 as well as \mathbf{n}' and \mathbf{B}_0 . Statistical isotropy is broken. Setting

$$\frac{\delta T}{T}(\mathbf{n}) = \sum_{l,m} a_{lm} Y_{lm}(\mathbf{n}), \quad (23)$$

in the isotropic situation, the C_l 's of Eq. (22) are just

$$C_l = \langle a_{lm} a_{lm}^* \rangle, \quad (24)$$

where $\langle \rangle$ denotes a theoretical expectation value over an ensemble of statistically identical universes. We find that the presence of the preferred direction \mathbf{B}_0 not only leads to an m -dependence of the correlators, but also induces correlations between the multipole amplitudes $a_{l+1,m}$ and $a_{l-1,m}$. Correlations in the temperature fluctuations at different points on the sky are no longer simply functions of their relative angular separation, but also of their orientations with respect to the external field. Detailed computations of the correlators for the Doppler contribution from Alfvén waves are presented in Appendix A. We obtain

$$\begin{aligned}
C_l(m) &= \langle a_{lm} a_{lm}^* \rangle \\
&= A_0 v_a^2 \left(\frac{t_{dec}}{t_0} \right)^2 (k_0 t_0)^{-(n+3)} \frac{2^{n+1} \Gamma(-n-1)}{\Gamma(-n/2)^2} \\
&\quad \times \left(\frac{2l^4 + 4l^3 - l^2 - 3l + 6m^2 - 2lm^2 - 2l^2 m^2}{(2l-1)(2l+3)} \right) \frac{\Gamma(l+n/2+3/2)}{\Gamma(l-n/2+1/2)}
\end{aligned} \tag{25}$$

$$\begin{aligned}
D_l(m) &= \langle a_{l-1,m} a_{l+1,m}^* \rangle = \langle a_{l+1,m} a_{l-1,m}^* \rangle \\
&= A_0 v_A^2 \left(\frac{t_{dec}}{t_0} \right)^2 (k_0 t_0)^{-(n+3)} \frac{2^{n+2} \Gamma(-n-1)}{|n+1| \Gamma(-(n+1)/2)^2} (l-1)(l+2) \\
&\quad \times \left(\frac{(l+m+1)(l-m+1)(l+m)(l-m)}{(2l-1)(2l+1)^2(2l+3)} \right)^{1/2} \frac{\Gamma(l+n/2+3/2)}{\Gamma(l-n/2+1/2)}.
\end{aligned} \tag{26}$$

This result is valid in the range $-7 < n < -1$. For $n \leq -7$ the quadrupole diverges at small k , and for $n > -1$ the result is dominated by the upper cutoff k_0 ,

$$C_l \approx D_l \approx \frac{v_A^2 A_0}{2\pi(n+1)(k_0 t_0)^2} \left(\frac{t_{dec}}{t_0} \right)^2 l^2, \quad n > -1. \tag{27}$$

For $n = -5$ we obtain a scale-invariant Harrison-Zeldovich spectrum, $C_l \sim l^2$.

To obtain some insight into the effect of the cross terms D_l , we picture the correlation function

$$f(\mathbf{n}) = \left\langle \frac{\delta T}{T}(\mathbf{n}_0) \frac{\delta T}{T}(\mathbf{n}) \right\rangle = \sum_{lm'l'm'} \langle a_{lm} a_{l'm'}^* \rangle Y_{lm}(\mathbf{n}_0) Y_{l'm'}^*(\mathbf{n}) \tag{28}$$

for various orientations of the magnetic field with respect to the fixed direction \mathbf{n}_0 . These are shown for the case $n = -5$ and with $\mathbf{n}_0 = \hat{\mathbf{z}}$ in Figs. 1–3. Notice, however, that these figures do not represent temperature maps but are plots of the correlation function. For a given realization stochastic noise has to be added. The explicit expression for $f(\mathbf{n})$ is given in Appendix A.

With no *a priori* knowledge of the field direction, it could be inferred by performing CMB measurements with various \mathbf{n}_0 and comparing the obtained $f(\mathbf{n})$ with the plots below. Of

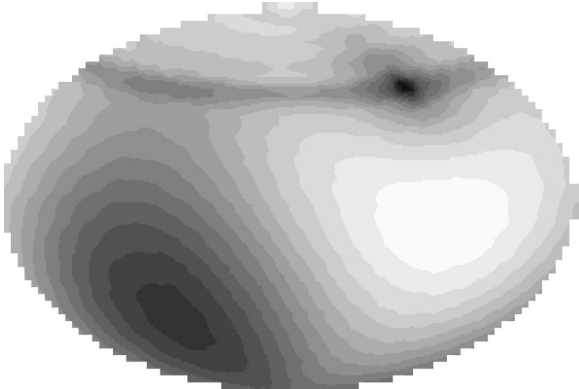


FIG. 1. An Aitoff projection of the function $f(\mathbf{n})$ for a homogeneous magnetic field pointing in the $\theta = \pi/4$, $\phi = \pi/2$ direction and the reference vector \mathbf{n}_0 pointing in the z -direction ($\theta = 0$) (see Eq. (28)).

course this procedure suffers from problems with cosmic variance, as once we fix a direction \mathbf{n}_0 in the sky we have only a single realization with which to determine f . The expectation value in expression (28), then, strictly refers to a (hypothetical) average over an ensemble of universes.

A probably simpler observational test of the existence of a constant magnetic field is the presence of temperature correlations for unequal l . To simplify, we introduce the mean values

$$\bar{C}_l = \overline{\langle a_{lm} a_{lm}^* \rangle}, \tag{29}$$

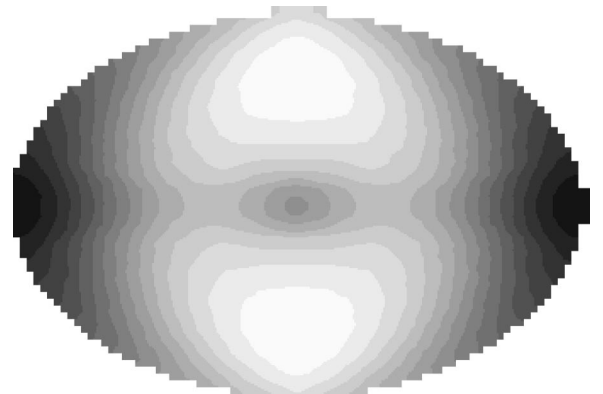


FIG. 2. The function $f(\mathbf{n})$ for \mathbf{B}_0 pointing in the $\theta = \pi/2$, $\phi = 0$ direction.



FIG. 3. The function $f(\mathbf{n})$ for \mathbf{B}_0 pointing in the $\theta=0$ direction (i.e., parallel to \mathbf{n}_0). The gray scale scheme has enhanced the variation in f .

$$\bar{D}_l = \overline{\langle a_{l-1,m} a_{l+1,m}^* \rangle}, \quad (30)$$

where the bar denotes average over different values of m , and we find

$$\begin{aligned} \bar{C}_l \approx & A_0 \left(\frac{t_{dec}}{t_0} \right)^2 (k_0 t_0)^{-(n+3)} \\ & \times v_A^2 \frac{2^{n+1} \Gamma(-n-1)}{3 \Gamma(-n/2)^2} l^{n+3}, \quad \text{for } n < -1 \end{aligned} \quad (31)$$

$$\bar{C}_l \approx A_0 \left(\frac{t_{dec}}{t_0} \right)^2 (k_0 t_0)^{-2} v_A^2 \frac{1}{n+1} l^2, \quad \text{for } n > -1 \quad (32)$$

$$\bar{D}_l / \bar{C}_l \approx 3/2. \quad (33)$$

The existence of significant correlations between the $a_{l-1,m}$ and $a_{l+1,m}$ is a clear indication of the presence of a preferred direction in the universe. Due to its spin-1 nature, a long-range vector field induces transitions $l \rightarrow l \pm 1$ and thus leads to the correlators D_l .

There are no published limits on these cross correlation terms. Since the full a_{lm} 's are needed to obtain such limits, full sky coverage and high resolution, as will be provided by the Microwave Anisotropy Probe (MAP) and PLANCK satellites, are most important. The galaxy cut in the 4-year COBE data leads to an influence of C_l by $C_{l \pm 2}$ which is on the order of 10% for $2 \leq l \leq 30$ [14]. It is not clear how much this galactic contribution will be reduced in future experiments. To be specific, let us assume that this is the limit on the off-diagonal correlations D_l . Then, first of all, the observed CMB anisotropies are not due to Alfvén waves, since $0.1 \approx D_l / C_l$ is substantially smaller than the figure in Eq. (33). To obtain a limit on the magnetic field amplitude and the spectral index, we now require

$$l^2 \bar{D}_l \leq 0.1 l^2 \bar{C}_l \approx 10^{-11} \quad \text{for } 2 < l \leq 100. \quad (34)$$

We now argue as follows. From Eq. (17), and the fact that $\mathbf{B}_1 \leq \mathbf{B}_0$, we have

$$|\mathbf{\Omega}_0|^2 k^3 \leq v_A^2. \quad (35)$$

This inequality must hold on all scales inside the horizon at decoupling, $k \geq 1/t_{dec}$. With Eq. (21) we therefore obtain

$$2A_0 (k/k_0)^{n+3} \leq v_A^2, \quad 1/t_{dec} \leq k \leq k_0, \quad (36)$$

which implies

$$2A_0 (k_0 t_{dec})^{-(n+3)} \leq v_A^2 \quad \text{for } n \leq -3, \quad (37)$$

$$2A_0 \leq v_A^2 \quad \text{for } n \geq -3. \quad (38)$$

Here we have identified k_0 with the maximal frequency (cut-off) of the magnetic field, which has to be introduced in the case $n > -3$ for $\mathbf{\Omega}$ not to diverge at small scales. A definite upper limit on k_0 is the scale beyond which the magnetic field is damped away, due to the finite value of the conductivity. The physical damping scale is given by [15]

$$(k_D/a)^2 = 4\pi\sigma/\tau, \quad (39)$$

where τ denotes the cosmic time (not comoving) and σ is the plasma conductivity. The conductivity of a non-relativistic electron-proton plasma is easily shown to be $\sigma \sim 4T$, and it has been shown recently that this result still holds approximately in the very early universe [16].

Using $T_{dec} \sim 0.3 \text{ eV} \sim 0.6 \times 10^{-4} \text{ cm}^{-1}$ and $\tau_{dec} \sim 10^5 \text{ yr} \sim 10^{23} \text{ cm}$, we obtain the comoving damping scale at decoupling

$$\begin{aligned} k_0(t_{dec}) \sim & k_D(t_{dec}) \sim (z_{dec})^{-1} \sqrt{16\pi T_{dec}/\tau_{dec}} \\ & \sim 3 \times 10^{-10} \text{ cm}^{-1}, \end{aligned} \quad (40)$$

and

$$\begin{aligned} (k_0 t_0)(t_{dec}) &= k_0(t_{dec}) \tau_0 / a_{dec} \\ &\sim \tau_0 \sqrt{16\pi T_{dec}/\tau_{dec}} \sim 0.4 \times 10^{14}. \end{aligned} \quad (41)$$

Inserting the limiting values of Eqs. (37), (38) for the A_0 in Eq. (31), Eq. (34) yields

$$3v_A^4 z_{dec}^{-(n+5)/2} \frac{2^{n+1} \Gamma(-n-1)}{3 \Gamma(-n/2)^2} l^{n+5} < 10^{-11} \quad \text{for } n < -3, \quad (42)$$

$$\begin{aligned} 3v_A^4 z_{dec}^{-1} (2.5 \times 10^{-14})^{(n+3)} \frac{2^{n+1} \Gamma(-n-1)}{3 \Gamma(-n/2)^2} l^{n+5} &< 10^{-11} \\ \text{for } -3 \leq n < -1, \end{aligned} \quad (43)$$

$$3v_A^4 z_{dec}^{-1} (2.5 \times 10^{-14})^2 \frac{1}{n+1} l^4 < 10^{-11} \quad \text{for } -1 < n. \quad (44)$$

Using $v_A \sim 4 \times 10^{-4} (B_0/10^{-9} \text{ G})$, this can be translated into a limit for B_0 which depends on the spectral index n and the harmonic l . In Fig. 4 we plot the best limit on B_0 as a function of the spectral index n . To optimize the limit we choose $l=2$ for $n < -5$ and $l=100$ for $n > -5$. For

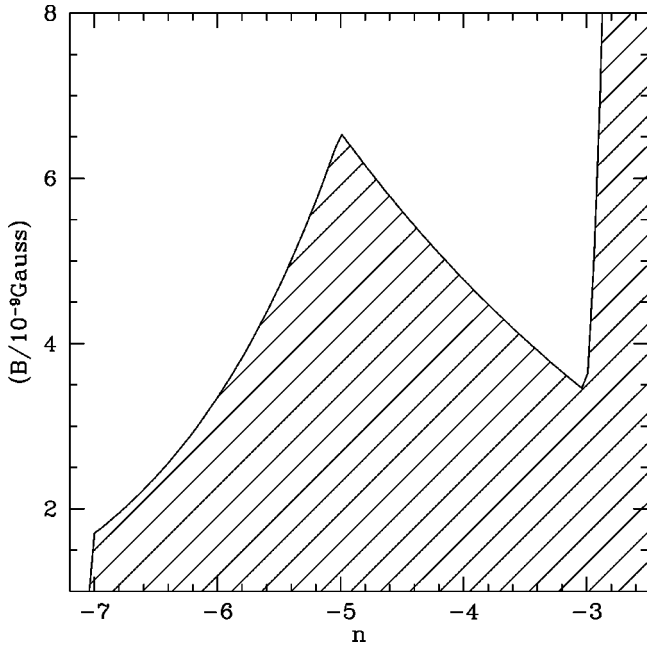


FIG. 4. The upper limit on the magnetic field amplitude B_0 due to CMB anisotropies caused by Alfvén waves, shown as a function of the magnetic field spectral index n . We assume $D_l \leq 0.1 C_l$. Allowed values of the field must lie in the dashed region.

$n > -3$ the limit rapidly becomes irrelevant due to the huge factor $10^{14(n+3)}$. This reflects the fact that for $n > -3$, the magnetic field fluctuations grow towards small scales, and $B_1 \leq B_0$ leads to a limit at the tiny scale $k = k_0$; whereas the CMB anisotropies are caused by the smaller fluctuations at large scales, $k \sim 1/t_0$. At $n \leq -1$ the induced D_l 's start to feel the upper cutoff and thus do not decrease any further.

The presence of a homogeneous magnetic field also induces anisotropic stresses in the metric. This gravitational effect has been estimated elsewhere [7]. Compared with the COBE DMR experiment, it leads to a similar limit for B_0 .

IV. CONCLUSIONS

We have studied Alfvén waves in the primordial electron-proton plasma that are sourced by a homogeneous magnetic field. In addition, we allow for an isotropic distribution of random magnetic fields on smaller scales. The induced vorticity in the baryon fluid leads, via the Doppler effect, to vector-type CMB anisotropies on all angular scales larger than the vectorial Silk damping scale $l_{damp} \sim 500$ (see Appendix B). The vector nature of the magnetic field induces off-diagonal correlations,

$$D_l(m) = \langle a_{l-1,m} a_{l+1,m}^* \rangle \sim C_l(m). \quad (45)$$

Assuming that observations constrain these terms to be less than about 10% of the observed C_l 's, we derive a limit for the amplitude of the magnetic field as a function of its spectral index. For $n < -7$, the quadrupole anisotropy diverges if no lower cutoff is imposed on the spectrum, and so such spectra are very strongly constrained. For $n > -3$, the con-

straint is proportional to $(k_0 t_0)^{(n+3)/4}$, where t_0 is the comoving scale today and k_0 is the upper cutoff of the spectrum. We have set $1/k_0$ equal to the magneto-hydrodynamical damping scale which is inversely proportional to the conductivity and thus extremely small, leading to $(k_0 t_0) \sim 10^{14}$. Therefore, the limits obtained for $n > -3$ are extremely weak and actually uninteresting. This is due to the fact that the quantity $B^2(k)k^3$ decreases on large scales for $n > -3$. For spectral indices in the range $-7 < n < -3$ the limit on B_0 is on the order of $(2-7) \times 10^{-9}$ G.

An important remark is also that causally induced magnetic fields lead to a spectral index $n=2$ and so are not constrained at all.² Examples here are magnetic fields generated by the decay of a Y field during the electroweak phase transition.

At first sight it may seem somewhat artificial to have split the magnetic field into a homogeneous component and an isotropic spectrum of random magnetic fields. However, this is the correct procedure for realistic observations. This is seen as follows. If we calculate the C_l 's for a given model, we determine expectation values over an ensemble of universes. If we make a measurement, however, we have just one observable universe at our disposition. This problem is generally referred to as ‘‘cosmic variance.’’ On scales much smaller than the horizon, cosmic variance is irrelevant if we make some kind of ergodicity hypothesis, assuming that spatial and ensemble averaging are equivalent. In the case here cosmic variance is especially important, however. If we include the field which is coherent on the horizon scale in our random distribution, then in performing the ensemble average we integrate over the directions of \mathbf{B}_0 and the off-diagonal correlators D_l vanish. The entire effect disappears. In one given universe, however, this field has one fixed direction and our effect is observable. It is therefore of fundamental importance here not to take an ensemble average over the large scale coherent field. Note however that the fluctuations induced by magnetic fields are non-Gaussian and even in the ensemble average the phenomenon discussed here would be visible but only in higher than second order correlators; see [17].

The cosmic variance problem is relevant whenever perturbations with non-vanishing power on horizon scales are present. An observational limit on the off-diagonal correlators D_l 's from MAP or PLANCK would represent a model-independent limit on the importance of large scale coherent vector fields (which enter quadratically in the energy momentum tensor) for the anisotropies in the cosmic microwave background. Its importance thus goes beyond the magnetic field case discussed in the present work.

²If we assume magnetic fields to be generated by a causal procedure, i.e. not during an inflationary epoch, in a Friedmann universe, then the real space correlation function has to vanish at super-horizon distances (say $|x| > 2t$). Its Fourier transform $\langle B_i B_j \rangle(\mathbf{k}) \propto k^n (\delta_{ij} - k_i k_j)$ is therefore analytic in \mathbf{k} , which requires n to be an integer with $n \geq 2$.

ACKNOWLEDGMENTS

It is a pleasure to acknowledge discussions with Kris Gorski, Alessandro Melchiorri and Misha Shaposhnikov. Francesco Melchiorri brought our attention to Ref. [14]. This work is financially supported by the Swiss NSF. T.K. is grateful for hospitality at Geneva University.

APPENDIX A: CALCULATION OF C_l FROM VECTOR PERTURBATIONS

In the usual way we decompose the temperature fluctuations of the microwave background into spherical harmonics:

$$\frac{\delta T}{T}(\mathbf{n}) = \sum_{lm} a_{lm} Y_{lm}(\mathbf{n}).$$

The two point function $\langle a_{lm} a_{l'm'}^* \rangle$ is then

$$\begin{aligned} \langle a_{lm} a_{l'm'}^* \rangle &= \frac{1}{(2\pi)^3} \int d^3k \int d\Omega_{\mathbf{n}} \int d\Omega_{\mathbf{n}'} \\ &\times \left\langle \frac{\delta T^*}{T}(\mathbf{n}, \mathbf{k}) \frac{\delta T}{T}(\mathbf{n}', \mathbf{k}) \right\rangle \\ &\times Y_{lm}^*(\mathbf{n}) Y_{l'm'}(\mathbf{n}'). \end{aligned} \quad (\text{A1})$$

We consider the contribution to the temperature anisotropy only from the vorticity in the baryon fluid. From Eq. (19), we obtain

$$\frac{\delta T}{T}(\mathbf{n}, \mathbf{k}, \Delta t) = e^{i\mathbf{k} \cdot \mathbf{n} \Delta t} \mathbf{n} \cdot \boldsymbol{\Omega}(\mathbf{k}, t_{dec}), \quad (\text{A2})$$

where $\Delta t = t_0 - t_{dec} \approx t_0$, the time elapsed since last scattering. Using the form (20) for the power spectrum of the vortical velocity fluctuations, we have

$$\langle a_{lm} a_{lm}^* \rangle = \left(\frac{2l^4 + 4l^3 - l^2 - 3l + 6m^2 - 2lm^2 - 2l^2m^2}{(2l-1)(2l+1)^2(2l+3)} \right) \frac{2}{\pi} \int dk k^2 (v_A k t_{dec})^2 A(k) (j_{l+1} + j_{l-1})^2 \quad (\text{A8})$$

and

$$\begin{aligned} \langle a_{l+1m} a_{l-1m}^* \rangle &= \langle a_{l-1m} a_{l+1m}^* \rangle \\ &= -(l-1)(l+2) \left(\frac{(l+m+1)(l-m+1)(l+m)(l-m)}{(2l-1)^3(2l+1)^2(2l+3)^3} \right)^{1/2} \\ &\times \frac{2}{\pi} \int dk k^4 (v_A t_{dec})^2 A(k) (j_l + j_{l-2})(j_l + j_{l+2}). \end{aligned} \quad (\text{A9})$$

The Bessel functions take kt_0 as their arguments. With $A(k) = A_0(k/k_0)^n k_0^{-3}$, we obtain, for $-7 < n < -1$,

$$\begin{aligned} \langle a_{lm} a_{lm}^* \rangle &\equiv C_l(m) \frac{2^{n+1} A_0 v_A^2}{(k_0 t_0)^{n+3}} \left(\frac{t_{dec}}{t_0} \right)^2 \frac{\Gamma(-n-1)}{\Gamma(-n/2)^2} \frac{\Gamma(l+n/2+3/2)}{\Gamma(l-n/2+1/2)} \\ &\times \frac{(2l^4 + 4l^3 - l^2 - 3l + 6m^2 - 2lm^2 - 2l^2m^2)}{(2l-1)(2l+3)}, \end{aligned} \quad (\text{A10})$$

$$\begin{aligned} &\left\langle \frac{\delta T^*}{T}(\mathbf{n}, \mathbf{k}) \frac{\delta T}{T}(\mathbf{n}', \mathbf{k}) \right\rangle \\ &= e^{i\mathbf{k} \cdot (\mathbf{n}' - \mathbf{n}) t_0} (\mathbf{n} \cdot \mathbf{n}' - \mu \mu') (v_A k \beta t_{dec})^2 A(k) \\ &= A(k) (v_A k \beta)^2 \left(e^{ikt_0(\mu' - \mu)} \mathbf{n} \cdot \mathbf{n}' \right. \\ &\quad \left. - \frac{\partial}{\partial(kt_0)} e^{-ikt_0\mu} \frac{\partial}{\partial(kt_0)} e^{ikt_0\mu'} \right) = f(\mathbf{n}, \mathbf{n}', \mathbf{k}), \end{aligned} \quad (\text{A3})$$

where $\mu = \mathbf{n} \cdot \hat{\mathbf{k}}$, $\mu' = \mathbf{n}' \cdot \hat{\mathbf{k}}$, $\beta = \mathbf{e} \cdot \hat{\mathbf{k}}$ and \mathbf{e} is the unit vector in the direction of the homogeneous magnetic field \mathbf{B}_0 . So

$$\begin{aligned} \langle a_{lm} a_{l'm'}^* \rangle &= \frac{1}{(2\pi)^3} \int d^3k \int d\Omega_{\mathbf{n}} \int d\Omega_{\mathbf{n}'} \\ &\times f(\mathbf{n}, \mathbf{n}', \mathbf{k}) Y_{lm}^*(\mathbf{n}) Y_{l'm'}(\mathbf{n}'). \end{aligned} \quad (\text{A4})$$

To evaluate these integrals, we use the identities

$$e^{i\mathbf{x} \cdot \hat{\mathbf{n}}} = 4\pi \sum_{r=0}^{\infty} \sum_{q=-r}^{+r} i^r j_r(x) Y_{rq}^*(\hat{\mathbf{k}}) Y_{rq}(\mathbf{n}), \quad (\text{A5})$$

$$\mathbf{n} \cdot \mathbf{n}' = P_1(\mathbf{n} \cdot \mathbf{n}') = \frac{4\pi}{3} \sum_{p=-1}^{+1} Y_{1p}(\mathbf{n}) Y_{1p}^*(\mathbf{n}'), \quad (\text{A6})$$

where j_r is the spherical Bessel function of order r . Using the orthonormality of the spherical harmonics and the recursion relation

$$(2l+1)j_l' = lj_{l-1} - (l+1)j_{l+1}, \quad (\text{A7})$$

we find that in evaluating Eq. (A4) only the terms with $(l, m) = (l', m')$ and $(l, m) = (l' \pm 2, m')$ survive, where

$$\begin{aligned}
\langle a_{l+1,m} a_{l-1,m}^* \rangle &= \langle a_{l-1,m} a_{l+1,m}^* \rangle \\
&\equiv D_l(m) \frac{2^{n+2} A_0 v_A^2}{|n+1| (k_0 t_0)^{n+3}} \left(\frac{t_{dec}}{t_0} \right)^2 \frac{\Gamma(-n-1)}{\Gamma(-(n+1)/2)^2} \frac{\Gamma(l+n/2+3/2)}{\Gamma(l-n/2+1/2)} \\
&\quad \times (l-1)(l+2) \left(\frac{(l+m+1)(l-m+1)(l+m)(l-m)}{(2l-1)(2l+1)^2(2l+3)} \right)^{1/2}. \tag{A11}
\end{aligned}$$

For $n > -1$ the integral is dominated by the upper cutoff k_0 and we find

$$C_l(m) = \frac{v_A^2 A_0}{2\pi(n+1)(k_0 t_0)^2} \left(\frac{t_{dec}}{t_0} \right)^2 \tag{A12}$$

$$\times \frac{(2l^4 + 4l^3 - l^2 - 3l + 6m^2 - 2lm^2 - 2l^2 m^2)}{(2l-1)(2l+3)}, \tag{A13}$$

$$D_l(m) = \frac{v_A^2 A_0}{2\pi(n+1)(k_0 t_0)^2} \left(\frac{t_{dec}}{t_0} \right)^2 \tag{A14}$$

$$\times (l-1)(l+2) \left(\frac{(l+m+1)(l-m+1)(l+m)(l-m)}{(2l-1)(2l+1)^2(2l+3)} \right)^{1/2}. \tag{A15}$$

In this case, the result is nearly independent of the spectral index n and, due to the factor $(k_0 t_0)^{-2}$, it is so small that it fails to lead to relevant constraints for B_0 .

The temperature correlation function is finally

$$\begin{aligned}
f(\mathbf{n}) &= \left\langle \frac{\delta T}{T}(\mathbf{n}_0) \frac{\delta T}{T}(\mathbf{n}) \right\rangle \\
&= \sum_{lm'l'm'} \langle a_{lm} a_{l'm'}^* \rangle Y_{lm}(\mathbf{n}_0) Y_{l'm'}^*(\mathbf{n}) \\
&= \sum_{lm} C_l(m) Y_{lm}(\mathbf{n}_0) Y_{lm}^*(\mathbf{n}) \\
&\quad + \sum_{lm} D_l(m) (Y_{l+1,m}(\mathbf{n}_0) Y_{l-1,m}^*(\mathbf{n}) \\
&\quad + Y_{l-1,m}(\mathbf{n}_0) Y_{l+1,m}^*(\mathbf{n})).
\end{aligned}$$

APPENDIX B: COLLISIONAL DAMPING FOR VECTOR PERTURBATIONS

Denoting the fractional perturbation in the radiation brightness by \mathcal{M} , $\mathcal{M} = 4(\Delta T/T)$, the Boltzmann equation for vector perturbations gives [11]

$$\begin{aligned}
\dot{\mathcal{M}} + \mathbf{n} \cdot \nabla \mathcal{M} &= -4n^i n^j \sigma_{i,j} + a\sigma_T n_e \\
&\quad \times [-\mathcal{M} + 4\mathbf{n} \cdot \mathbf{\Omega}]. \tag{B1}
\end{aligned}$$

Here \mathbf{n} is the photon direction, σ_T denotes the Thomson cross section and $\mathbf{\Omega}$ is the baryon vorticity. We have neglected the anisotropy of non-relativistic Compton scattering.

To the baryon equation of motion (8) we have to add the photon drag force,

$$\dot{\mathbf{\Omega}} + \frac{\dot{a}}{a} \mathbf{\Omega} = \frac{a\sigma_T n_e \rho_r}{3\rho_b} \left[\frac{1}{4} \mathbf{M} - \mathbf{\Omega} \right], \tag{B2}$$

with

$$\mathbf{M} = \frac{3}{4\pi} \int \mathbf{n} \mathcal{M} d\mathbf{n}.$$

We shall also use the fact that for vector perturbations, the perturbation of the photon brightness vanishes,

$$\int \mathcal{M} d\mathbf{n} = 0.$$

Due to the loss of free electrons during recombination, the mean (conformal) collision time $t_c = 1/(a\sigma_T n_e)$ increases from a microscopically small scale before recombination to a super-horizon scale after recombination. After recombination the collision term can be neglected and we recover Eqs. (8) and (18). We first consider the very tight coupling regime, $t_c \ll \lambda$, where λ denotes the typical scale of fluctuations. In this limit the term inside the square brackets of Eqs. (B1) and (B2) can be set to zero and we obtain $\mathbf{M} = 4\mathbf{\Omega}$ (the baryon and photon fluids are adiabatically coupled).

Next, we derive a dispersion relation for the damping of fluctuations due to the finite size of t_c . We proceed in the same way as Peebles [18] for scalar perturbations. We consider scales with wavelength $k^{-1} \ll t$ and thus neglect the time dependence of the coefficients in Eqs. (B1) and (B2). To study the damping we also neglect gravitational effects, which act on much slower timescales. With the ansatz

$$\mathcal{M} = \mathcal{A}(\mathbf{n}) \exp(i(\mathbf{k}\mathbf{x} - \omega t)), \quad (\text{B3})$$

$$\mathcal{Q} = \mathcal{B}(\mathbf{n}) \exp(i(\mathbf{k}\mathbf{x} - \omega t)), \quad (\mathcal{B} \cdot \mathbf{k}) = 0 \quad (\text{B4})$$

we obtain

$$-i\omega\mathcal{A} + i(\mathbf{k}\mathbf{n})\mathcal{A} = \frac{1}{t_c} [-\mathcal{A} + 4\mathbf{n} \cdot \mathcal{B}] \quad (\text{B5})$$

$$-i\omega\mathcal{B} = \frac{1}{t_c R} [\mathbf{M} - 4\mathcal{B}], \quad R \equiv \frac{3\rho_b}{4\rho_\gamma}. \quad (\text{B6})$$

In the limit $kt_c, \omega t_c \rightarrow 0$, we again obtain adiabatic coupling. The general relation between \mathcal{A} and \mathcal{B} is

$$\mathcal{A} = \frac{4\mathbf{n} \cdot \mathcal{B}}{1 + i(\mathbf{k} \cdot \mathbf{n} - \omega)t_c}$$

and so

$$\mathbf{M} = 3\mathcal{B} \frac{i}{(kt_c)^3} \left[-((kt_c)^2 + (1 - i\omega t_c)^2) \times \ln \left(\frac{1 - it_c(\omega - k)}{1 - it_c(\omega + k)} \right) + 2ikt_c(1 - i\omega t_c) \right]. \quad (\text{B7})$$

Inserting this in Eq. (B6) leads again, in the limit $kt_c, \omega t_c \rightarrow 0$, to the tight coupling result. In first order kt_c [the square bracket in Eq. (B7) has to be expanded up to order $(kt_c)^5$] we obtain the dispersion relation

$$\omega = -i\gamma, \quad \text{with } \gamma = \frac{7k^2 t_c}{20(1+R)} \sim \frac{k^2 t_c}{3}. \quad (\text{B8})$$

In contrast to the scalar case, vector perturbations show no oscillations [$\text{Re}(\omega) = 0$] but are just damped. The damping occurs at a slightly larger scale than for scalar perturbations, where $\gamma_{\text{scalar}} \approx k^2 t_c / 6$ [18].

The ratio $R = 3\rho_b / (4\rho_\gamma)$ is smaller than $\sim 1/4$ until the end of recombination. We therefore obtain a damping factor f for a given scale k

$$f \sim \exp \left(\frac{7k^2}{20} \int_0^{t_{\text{end}}(k)} t_c dt \right), \quad (\text{B9})$$

where $t_{\text{end}}(k)$ is the time at which our approximation $kt_c < 1$ breaks down, i.e., $kt_c(t_{\text{end}}(k)) = 1$. The time over which the damping is active is the order of the thickness of the last scattering surface, $\Delta t \sim t_{\text{dec}} (\Delta z / z_{\text{dec}}) \sim 0.1 t_{\text{dec}}$. The damping scale, the scale at which the exponent in Eq. (B9) becomes of order unity, is about

$$k_{\text{damp}} t_{\text{dec}} \sim 10. \quad (\text{B10})$$

The harmonic l corresponding to k_{damp} is $l_{\text{damp}} = k_{\text{damp}} t_0 \sim 10 t_0 / t_{\text{dec}} \sim 500$.

After the time $t_{\text{end}}(k)$, collisions become unimportant for fluctuations with wave number k which then evolve freely, suffering only directional dispersion which induces a power law damping $\propto 1/(k\Delta t)$. Reference [8] discusses only this second effect. Numerical experience with scalar perturbations, however, shows that they are typically both of similar importance.

-
- [1] G. Smoot *et al.*, *Astrophys. J. Lett.* **396**, L1 (1992).
[2] W. Hu, N. Sugiyama, and J. Silk, *Nature (London)* **386**, 37 (1997); W. Hu and M. White, *Astrophys. J.* **471**, 30 (1996).
[3] C. M. Ko and E. N. Parker, *Astrophys. J.* **341**, 828 (1989); S. I. Vainshtein and R. Rosner, *ibid.* **376**, 199 (1991); F. Cattaneo, *ibid.* **434**, 200 (1994); A. V. Gruzinov and P. H. Diamond, *Phys. Rev. Lett.* **72**, 1651 (1994).
[4] M. Gasperini, M. Giovannini, and G. Veneziano, *Phys. Rev. Lett.* **75**, 3796 (1995); D. Lemoine and M. Lemoine, *Phys. Rev. D* **52**, 1955 (1995).
[5] M. Giovannini and M. Shaposhnikov, *Phys. Rev. Lett.* **80**, 22 (1998).
[6] J. Adams, U. H. Danielsson, D. Grasso, and H. Rubinstein, *Phys. Lett. B* **388**, 253 (1996).
[7] J. Barrow, P. Ferreira, and J. Silk, *Phys. Rev. Lett.* **78**, 3610 (1997).
[8] K. Subramanian and J. Barrow, *Phys. Rev. Lett.* **81**, 3575 (1998).
[9] E. Kim, A. Olinto, and R. Rosner, *Astrophys. J.* **468**, 28 (1996).
[10] H. Kodama and M. Sasaki, *Prog. Theor. Phys. Suppl.* **78**, 1 (1984).
[11] R. Durrer, *Fundam. Cosm. Phys.* **15**, 209 (1994).
[12] J. Silk, *Astrophys. J.* **151**, 459 (1968).
[13] R. Durrer and N. Straumann, *Helv. Phys. Acta* **61**, 1027 (1988).
[14] E. L. Wright *et al.*, *Astrophys. J. Lett.* **464**, L21 (1996).
[15] See, for example, *Classical Electrodynamics*, 2nd ed., edited by J. D. Jackson (Wiley, New York, 1972).
[16] J. Ahonen and K. Enqvist, *Phys. Lett. B* **382**, 40 (1996).
[17] P. Ferreira and J. Maguejo, *Phys. Rev. D* **56**, 4578 (1997).
[18] P. J. E. Peebles, *The Large-Scale Structure of the Universe* (Princeton University Press, Princeton, NJ, 1980).